

## Spaceborne low light imaging based on EMCCD and CMOS

Wu Xingxing, Liu Jinguo, Zhou Huaide, Zhang Boyan

(Changchun Institute of Optics, Fine Mechanics and Physics, Chinese Academy of Sciences, Changchun 130033, China)

**Abstract:** Electron Multiplying Charge Coupled Device (EMCCD) can realize read out noise of less than  $1e^-$  by promoting gain of charges with the charge multiplication principle and is suitable for low light imaging. With the development of back illuminated CMOS technology CMOS with high quantum efficiency and less than  $1.5e^-$  read noise has been developed by Changchun Institute of Optics, Fine Mechanics and Physics(CIOMP). Spaceborne low light detection cameras based on EMCCD CCD201 and based on CMOS were respectively established and system noise models were founded. Low light detection performance as well as principle of spaceborne camera based on EMCCD and spaceborne camera based on CMOS were compared and analyzed. Results of analysis indicate that signal to noise (SNR) of spaceborne low light detection camera based on EMCCD will be 23.78 as radiance at entrance pupil of the camera is as low as  $10^{-9} \text{ W} \cdot \text{cm}^{-2} \cdot \text{sr}^{-1} \cdot \mu\text{m}^{-1}$  at the focal plane temperature of  $20^\circ\text{C}$ . Spaceborne low light detection camera worked in starring mode and the integration time is 2 s. SNR of low light detection camera based on CMOS will be 27.42 under the same conditions. If cooling systems are used and the temperature is lowered from  $20^\circ\text{C}$  to  $-20^\circ\text{C}$ , SNR of low light detection camera based on EMCCD will be improved to 27.533 while SNR of low light detection camera based on CMOS will be improved to 27.79.

**Key words:** space camera; low light; EMCCD; CMOS

**CLC number:** V445.8 **Document code:** A **DOI:** 10.3788/IRLA201645.0514002

## 基于 EMCCD 和 CMOS 的天基微光成像

武星星, 刘金国, 周怀得, 张博研

(中国科学院长春光学精密机械与物理研究所, 吉林 长春 130033)

**摘要:** 电子倍增电荷耦合器件(EMCCD)利用电荷雪崩机制可以实现低于  $1e^-$  的读出噪声,适用于微光成像。随着背照式 CMOS 成像探测器技术的发展,具有高量子效率和低于  $1.5e^-$  读出噪声的 CMOS 成像探测器已中国科学院长春光学精密机械与物理研究所研制成功。针对天基微光成像的需求,分别构建了基于 EMCCD CCD201 的天基微光相机和基于 CMOS 的天基微光相机,并建立了系统的噪声模型。对基于 EMCCD 的天基微光相机和基于 CMOS 的天基微光相机的微光探测性能和工作机理进行了对比分析。分析结果表明:当采用凝视成像模式,积分时间为 2 s,相机入瞳辐亮度为  $10^{-9} \text{ W} \cdot \text{cm}^{-2} \cdot \text{sr}^{-1} \cdot \mu\text{m}^{-1}$  时,基于 EMCCD 的天基微光相机在焦面温度为  $20^\circ\text{C}$  的条件下的信噪比为

收稿日期:2015-09-18; 修订日期:2015-10-30

基金项目:国家自然科学基金(61108066);吉林省科技发展计划(20130101028jc)

作者简介:武星星(1980-),男,研究员,博士,主要从事空间遥感成像技术等方面的研究。Email:starglare@126.com

23.78, 相同条件下基于 CMOS 的天基微光相机的信噪比为 27.42。当采用制冷系统将焦面温度降低至 -20℃ 时, 基于 EMCCD 的天基微光相机的信噪比提高到 27.533, 而基于 CMOS 的天基微光相机的信噪比提高到 27.79。

关键词: 空间相机; 微光; EMCCD; CMOS

## 0 Introduction

Traditional space-borne visible band cameras take photograph of objects on earth only under entertain sun light conditions such as sun zenith angle is among  $[20^\circ, 70^\circ]$ <sup>[1]</sup>. So imaging time is limited (commonly 8:30 - 17:30) in 24 hours of one day. Other time is so called "leak of time". Space-borne low light imaging camera is capable of imaging under moon light or star light and obtains visible band information of objects at all times<sup>[2]</sup>. In this way the problem of "leak of time" can be solved. It is especially useful for detection of low cloud and fog at night which cannot be detected by infrared camera<sup>[3-4]</sup>. Space-borne low light imaging camera can also obtain images of artificial lights on the surface of the earth which is very useful for monitoring human activities and urban research<sup>[5]</sup>.

Operational Linescan System (OLS) on DSMP satellite is a typical space-borne low light imaging camera. OLS is based on photomultiplier tube (PMT) and can detect radiance as low as  $10^{-9} \text{ W/cm}^2/\text{sr}/\mu\text{m}$ <sup>[6]</sup>. Spatial resolution of OLS is 2.7km. Electron Multiplying Charge Coupled Device (EMCCD) can realize read out noise of less than 1e- by promoting gain of charges with the charge multiplication principle and is suitable for low light imaging<sup>[7]</sup>. EMCCD doesn't need complicated image intensifier and hundreds volts of driving voltages of ICCD<sup>[8]</sup>. So it is suitable for space application. Low light night vision cameras based on ICCD, EBCCD and EMCCD has been developed and used in civil and military applications<sup>[9]</sup>. PMT was first used in spaceborne low light detection camera (OLS) on DSMP satellite. However it had drawbacks such as low reliability, larger size and being heavy.

Spaceborne low light detection camera based on EMCCD was developed for tridimensional imaging of low clouds and heavy fogs at night<sup>[10]</sup>. Latest low light detection cameras having been developed were mostly based on EMCCD. However EMCCD has the problem of gain aging<sup>[11]</sup>. Gain will fall off at a fixed voltage and temperature.

CMOS with high sensitivity and less than 1.5e-read noise has been developed by subordinate enterprise of Changchun Institute of Optics, Fine Mechanics and Physics (CIOMP).

In this paper, spaceborne low light detection cameras based on EMCCD CCD201 and based on CMOS were respectively established and system noise models were founded. Low light detection performance of spaceborne camera based on EMCCD and spaceborne camera based on CMOS were compared and analyzed.

## 1 Working principle of spaceborne low light imaging camera

Working pinciple of spaceborne low light imaging camera is as Fig.1 shows. Spaceborne low light imaging camera is composed of optical lens module, two dimentional moving frames and image motion compensation module.

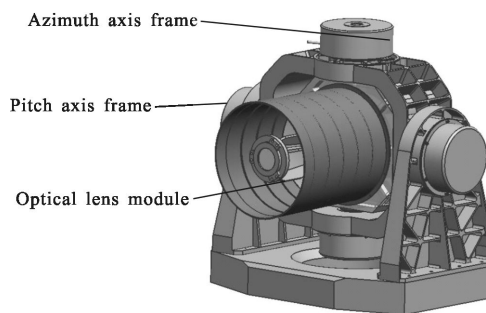


Fig.1 Working principle of space-borne low light imaging camera

Catadioptric optical lens module was mounted on two dimensional moving frames driven by brushless DC motors. Fast steering mirrors were used in image motion compensation module to compensate image motion caused by along-orbit motion of satellite and motion of moving frames [12]. Spectral range of the space-borne low light imaging camera is 500–900 nm which is the same as spectral range of OLS.

Spaceborne low light imaging camera can work both in general survey mode and in staring mode. Figure 2 shows staring mode of space-borne low light imaging camera. In general survey mode pitch axis frame keep still and pitch axis frame moves back and forth to realize rather wide continuous coverage. In staring mode azimuth axis frame and pitch axis frame move together to make the optical lens module stare at the objective district for a long time. In this way longer integration time than general survey mode can be realized and lower radiance can be detected.

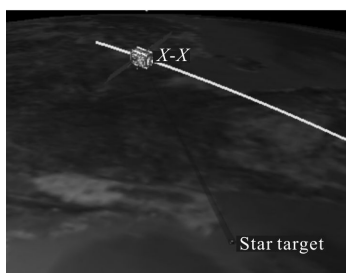


Fig.2 Staring mode of space-borne low light imaging camera

The maximum integration time in staring mode can be 5 seconds. In this paper integration time 2 s was used to compare low light imaging performance of low light imaging camera based on EMCCD and that of low light imaging camera based on CMOS.

SNR of camera is related to parameters of both optical system and sensor's photoelectric performance.  $F$  number of catadioptric optical lens module was designed to be 2. Transmission ratio of the whole optical system was 0.8.

## 2 Spaceborne low light imaging camera based on EMCCD

In this paper CCD201–20 of E2V company was

used in spaceborne low light imaging camera based on EMCCD. CCD201–20 has 1024 (H) × 1024 (V) active pixels which size is 13 μm × 13 μm. CCD201–20 can work in normal mode and in high gain mode. In normal mode readout noise at pixel rate of 15 MHz would be 43 e<sup>-</sup>. In high gain mode as voltage of multiplication phase amplitude  $R\Phi 2$  HV varies from 39 to 46 V, multiplication gain changes from 1 to 1 000. Figure 3 shows sketch of spaceborne low light imaging camera based on EMCCD.

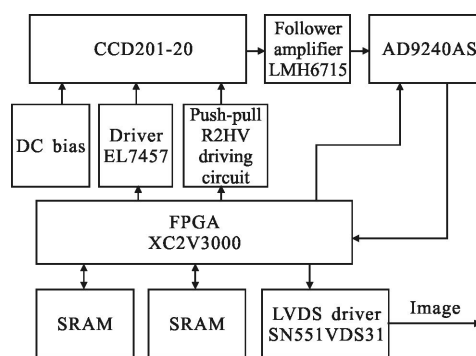


Fig.3 Sketch of spaceborne low light imaging camera based on EMCCD

Follower amplifier LMH6715 was used for impedance matching of analog output of CCD201–20. AD9240AS was used as A/D converter to convert analog output into digital numbers. Push-pull driving circuit was used to generate  $R\Phi 2$  HV driving voltage. MOSFET driver EL7457 can work at 40 MHz with output voltage ranging from –5 to 16 V. So it was used as driver to generate horizontal and vertical transfer driving signal. FPGA XC2V3000 produced control signals for CCD201–20 and processed digital numbers from AD9240AS. Digital numbers were stored into SRAM sequentially to form a frame of picture. In order to send output image in high speed for a long distance LVDS driver SN55LVDS31 was used to convert TTL signals into low voltage differential signals.

Noise sources of space-borne low light imaging camera based on EMCCD include readout noise, dark current noise, shot noise, additional noise caused by

charge multiplication process and clock induced charge noise<sup>[13]</sup>. Additional noise caused by charge multiplication process is usually calculated with noise factor. Signal to noise (SNR) of space-borne low light imaging camera based on EMCCD is as Eq.(1) shows:

$$SNR_{EMCCD} = \frac{D_{QE} \cdot P}{\sqrt{F^2 \cdot (D_{QE} \cdot P + \delta_{dark}^2 + \delta_{cic}) + \frac{\delta_{readout}^2}{M^2}}} \quad (1)$$

Where  $D_{QE}$  is quantum efficiency of EMCCD,  $P$  is photon number,  $F$  is noise factor ( $\sqrt{2}$  for CCD201-20),  $\delta_{dark}$  is dark current noise,  $\delta_{cic}$  is clock induced charge noise,  $\delta_{readout}$  is readout noise and  $M$  is multiplication gain.

Figure 4 shows variation of dark signal with temperature. In starring mode and the integration time was 2 second. As radiance at entrance pupil of the camera was as low as  $10^{-9} W \cdot cm^{-2} \cdot sr^{-1} \cdot \mu m^{-1}$ , SNR of space-borne low light imaging camera based on EMCCD would be 23.78 at the focal plane temperature of 20 °C.

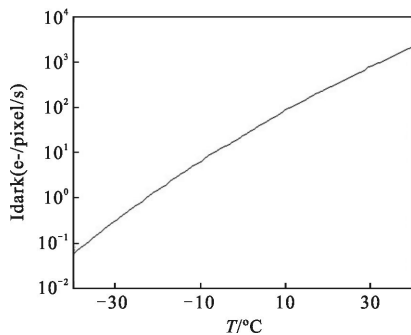


Fig.4 Variation of dark signal with temperature

If cooling system was equipped and temperature was lowered to -20 °C, SNR of the camera would be 27.533.

### 3 Spaceborne low light imaging camera based on CMOS

Back illuminated image sensors can realize higher quantum efficiency than front illuminated image sensors<sup>[14]</sup>. Back illuminated CMOS Imager GSENSE400BSI developed by CIOMP was used in spaceborne low light imaging camera based on

CMOS. GSENSE400BSI is as Figure 5 shows. Peak quantum efficiency of visible band of GSENSE400BSI is 90% @400 nm.

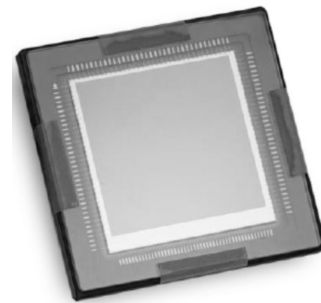


Fig.5 GSENSE400BSI

With latest back illuminated CMOS technology readout noise of GSENSE400BSI is as low as 1.3 e-. Figure 6 shows sketch of spaceborne low light imaging camera based on CMOS.

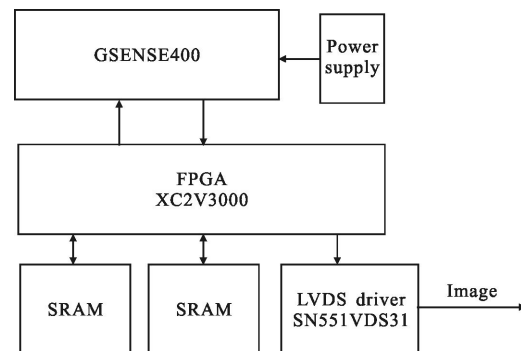


Fig.6 Sketch of spaceborne low light imaging camera based on CMOS

CMOS doesn't need high driving voltage of EMCCD so driver circuits like EL7457 are no more needed. FPGA XC2V3000 was used to generate complicated control signals of GSENSE400BSI. As AD converter and readout circuit are embedded in CMOS imager Output of Gsense400BSI in digital form could be directly processed by XC2V3000. Two SRAM chips were used to form ping-pang cache structure for high speed image process. Digital images were converted into differential signals for long-distance transmission by LVDS driver SN55LVDS31. Noise sources of low light imaging camera based on CMOS include readout noise, dark current noise and

shot noise. Here readout noise represents noise other than dark current noise and shot noise including A/D conversion noise, etc. SNR of space-borne low light imaging camera based on CMOS is as Eq.(2) shows:

$$SNR_{cmos} = \frac{S}{\sqrt{S + \delta_{dark}^2 + \delta_{readout}^2}} \quad (2)$$

Where  $S$  is photoelectron number,  $\delta_{dark}$  is dark current noise and  $\delta_{readout}$  is readout noise. It can be seen from Eq.(2) that noise model of CMOS is much simpler than noise model of EMCCD. Figure 7 shows change of quantum efficiency along with wavelength. Obviously peak quantum efficiency is obtained at 400 nm and quantum efficiency falls quickly at near-infrared band and at near ultraviolet band.

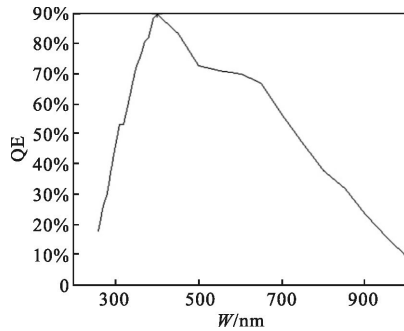


Fig.7 Change of quantum efficiency along with wavelength

As spaceborne low light imaging camera based on CMOS worked in starring mode and the integration time was 2 second. At the same time radiance at entrance pupil of the camera was as low as  $10^{-9} W \cdot cm^{-2} \cdot sr^{-1} \cdot \mu m^{-1}$ . SNR of space-borne low light imaging camera based on CMOS would be 27.42 at the focal plane temperature of 20 °C.

Dark current noise of GSENSE400 at 20 °C is about  $11e^{-}/s/pix$ . If cooling system was equipped and temperature was lowered to -20 °C, dark current noise would be  $0.4e^{-}/s/pix$ . SNR of spaceborne low light imaging camera based on CMOS would be 27.79. As photoelectron number is directly proportional to integration time. Mathematic relationship of SNR and integration time  $T_i$  can be expressed by Eq.(3).

$$SNR_{cmos} = \frac{K \cdot T_i}{\sqrt{K \cdot T_i + \delta_{dark}^2 + \delta_{readout}^2}} \quad (3)$$

Figure 8 shows change curves of SNR along

with integration time based on EMCCD and CMOS.

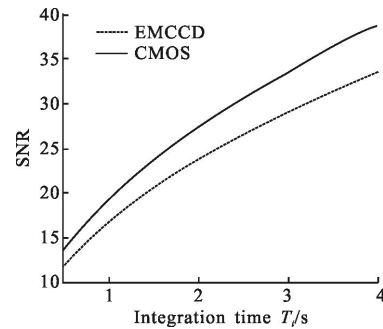


Fig.8 Change curves of SNR along with integration time based on EMCCD and CMOS

It can be seen from Fig.8 that with the increase of integration time both SNR of low light camera based on EMCCD and SNR of low light camera based on CMOS would be improved. Generally higher SNR could be obtained by low light camera based on CMOS with the same integration time.

Merits and drawbacks can be deduced by comparing low light detection performance as well as principle of spaceborne low light imaging camera based on CMOS and spaceborne low light imaging camera based on EMCCD. Cooling system for spaceborne low light imaging camera based on CMOS may not be needed. As a result power dissipation, weight and money can be saved. In addition system is simpler and reliability can be improved.

Another advantage of spaceborne low light imaging camera based on CMOS is better total dose irradiation endurance ability under space circumstance. Quantitative remote sensing can be realized conveniently as no gain aging effects need to be taken into consideration.

## 4 Conclusion

In order to solve "leak of time" problem of traditional space-borne visible band camera, spaceborne low light detection cameras based on EMCCD CCD201 and based on CMOS were respectively established and system noise models were founded. Low light detection performance as well as

principle of spaceborne camera based on EMCCD and spaceborne camera based on CMOS were compared and analyzed.

Results of analysis indicated that signal to noise (SNR) of spaceborne low light detection camera based on EMCCD would be 23.78 as radiance at entrance pupil of the camera was as low as  $10^{-9} \text{ W} \cdot \text{cm}^{-2} \cdot \text{sr}^{-1} \cdot \mu\text{m}^{-1}$  at the focal plane temperature of  $20 \text{ }^\circ\text{C}$ . Spaceborne low light detection camera worked in starring mode and the integration time was 2 second. SNR of low light detection camera based on CMOS would be 27.42 under the same conditions. If cooling systems were used and the temperature was lowered from  $20 \text{ }^\circ\text{C}$  to  $-20 \text{ }^\circ\text{C}$ , SNR of low light detection camera based on EMCCD would be improved to 27.533 while SNR of low light detection camera based on CMOS would be improved to 27.79. Cooling system for spaceborne low light imaging camera based on CMOS can be canceled to save power dissipation, weight and money. In addition reliability can be improved and gain aging problem of EMCCD can be avoided.

### References:

- [1] Wu Xingxing, Liu Jinguo, Zhou Huaide, et al. Automatic on-orbit adjusting gains of space camera based on lighting conditions [J]. *Acta Optica Sinica*, 2014, 34(3): 0328001-1-7. (in Chinese)
- [2] Guo Hui, Xiang Shiming, Zhang Feng. A review of the development of low-light night vision technology [J]. *Infrared Technology*, 2013, 35(2): 63-68. (in Chinese)
- [3] Yang Shaokui, Liu Wen. Color fusion method for low-level light and infrared images [J]. *Infrared and Laser Engineering*, 2014, 43(5): 1654-1659. (in Chinese)
- [4] Deng Chan, Liu Wen, Huang Biao. Color fusion system of low-light level and infrared images based on multi-core DSP [J]. *Infrared and Laser Engineering*, 2014, 43 (9): 3141-3145. (in Chinese)
- [5] Husi Letu, Masanao Hara, Gegen Tana. A saturated light correction method for DMSP/OLS nighttime satellite imagery [J]. *IEEE Transactions on Geoscience and Remote Sensing*, 2012, 50(2): 389-396..
- [6] Koel Roychowdhury, Simon D Jones, Colin Arrowsmith, et al. A comparison of high and low gain DMSP/OLS satellite images for the study of socio-economic metrics [J]. *IEEE Journal of Selected Topics in Applied Earth Observations and Remote Sensing*, 2011, 4(1):35-42.
- [7] Zhang Lei, Shi Feng, Zou Yan, et al. Method and experiment of photon counting imaging based on EMCCD [J]. *Infrared and Laser Engineering*, 2015, 44 (1): 384-390. (in Chinese)
- [8] Lian Mindong, Wang Shitao. Research on the imaging performance of space low light level imaging system based on ICCD [J]. *Spacecraft Recovery & Remote Sensing*, 2007, 28(3): 6-10. (in Chinese)
- [9] Chen Min, Yang Shengjie. Performance analysis and application of EMCCD [J]. *Electronics Optics & Control*, 2009, 16(1): 48-50. (in Chinese)
- [10] Hu Xiaohua, Zhou Xiaozhong, Liu Songtao, et al. Spaceborne shimmer tridimensional imaging technology and its implementation[J]. *Chinese Optics*, 2013, 6(5): 701-709. (in Chinese)
- [11] Smith David R, Waltonb David M, Richard Ingleya, et al. EMCCDs for space applications [C]//SPIE, 2006, 62760: 62760K-1-12.
- [12] Xu Xinhang, Yang Hongbo, Wang Bing. Research on key technology of fast-steering mirror [J]. *Laser & Infrared*, 2013, 43(10): 1095-1103.
- [13] Antoinette O'Grady. A comparison of EMCCD, CCD and emerging technologies optimized for low light spectroscopy applications[C]//SPIE, 2006, 6093: 60930S-1-9.
- [14] Alper Ercan, Kyriaki Minoglou. A model to estimate QE/MTF of thinned, back-side illuminated image sensors [J]. *Optical and Quantum Electronics*, 2015, 47(5): 1267-1282.